Vol. 453: 137–149, 2012
doi: 10.3354/meps09623

MARINE ECOLOGY PROGRESS SERIES
Mar Ecol Prog Ser

Published May 7

Surface-sediment bioturbation quantified with cameras on the NEPTUNE Canada cabled observatory

K. Robert[1,*], S. K. Juniper[1,2]

[1]Department of Biology, University of Victoria, PO Box 3020, STN CSC, Victoria, British Columbia V8W 3N5, Canada
[2]School of Earth and Ocean Sciences, University of Victoria, PO Box 3065, STN CSC, Victoria, British Columbia V8W 3V6, Canada

ABSTRACT: The mixing of deep-sea sediments by benthic megafauna is an important ecological service that influences biogeochemical processes. Quantifying the contribution of individual species to bioturbation and their responses to environmental variations requires experimental manipulation or direct observation, both of which are logistically challenging in the deep sea. Emerging cabled seafloor observatories now permit real-time data transfer to shore and interactive sampling, providing a new tool for long-term studies of the benthos at high temporal resolutions. We report on the development of a methodological approach to study surficial bioturbation by megafauna in a submarine canyon by using video cameras remotely operated over the internet, through the NEPTUNE Canada observatory. Observation protocols and image analysis techniques were developed to quantify organism size, locomotion and appearance rates for 2 flatfishes (Dover sole *Microstomus pacificus* and Pacific halibut *Hippoglossus stenolepis*) and the fragile pink sea urchin *Allocentrotus fragilis*. Application of a Bayesian model to extrapolate megafaunal locomotion patterns and appearance rates yielded sediment-surface reworking rates on the order of 26.0 to 35.1 $cm^2\ yr^{-1}$. Future observations can be directly incorporated into the model to improve accuracy. We propose that this combined observation and Bayesian modeling approach could become a useful component of a long-term program for monitoring ecological processes on the seafloor.

KEY WORDS: Bioturbation · Megafauna · Cabled observatories · Camera systems · Protocol development · Bayesian modeling

INTRODUCTION

The floor of the deep ocean, arguably the most extensive habitat on earth, remains markedly understudied particularly with regard to phenomena requiring long-term observations. Deploying instruments and cameras in the deep sea for time-series studies is costly and logistically challenging. Time-lapse camera deployments have provided some key insights into the functioning and dynamics of deep-sea ecosystems. For example, they have been used to describe the role of scavengers and carcass falls (Witte 1999) in deep-sea food webs and ecosystem responses to seasonal inputs of phytodetritus (Lampitt et al. 2001, Smith et al. 2008). Another important deep-sea ecosystem process that can be studied in time-series imagery is bioturbation, the mixing of sediment by benthic organisms (K. L. Smith et al. 1993, Kaufmann & Smith 1997, Bett et al. 2001, Belley et al. 2010). Deposit-feeders ingest sediments, absorb their organic content and excrete pellets. Burrowing organisms, through bioirrigation and vertical mixing of particles (Meysman et al. 2006), directly alter sediment properties both physically (Rhoads & Boyer 1982) and chemically (Aller 1982). Although bioturbation estimates for the deep sea are available (Teal

*Email: katleenr@uvic.ca

et al. 2008, Lecroart et al. 2010), they remain spatially limited and many regions of the deep sea, such as the one in the present study, remain to be examined.

Bioturbation has most commonly been studied through the use of vertical tracers or time-lapse imagery. In the former, natural or artificial tracers deposited on the surface are eventually buried deeper within the sediment column as a result of faunal activity (Maire et al. 2008). Sediment cores are then taken and sliced. A mathematical model is fitted to the resulting profile of tracer quantity over depth to yield biodiffusion coefficients (D_b) or mixed layer depth (L) (Meysman et al. 2008b). Naturally occurring tracers, such as radionuclides (C. B. Smith et al. 1993, Gerino et al. 1998), or artificially introduced tracers, such as luminophores or isotopically labelled particles (Bradshaw et al. 2006, Maire et al. 2006), have been used to resolve different timescales of vertical mixing of sediments. Regardless of the tracer method used, the obtained D_b only provides a time-averaged estimate of bioturbation. Although limited to the observation of larger organisms moving over the sediment surface, time-series image analysis does allow a better resolution of short-term processes (Maire et al. 2008) and ensures that we can observe the actual organisms responsible for sediment bioturbation and partition their contributions. This approach has been used to quantify bioturbation in imagery obtained with autonomous cameras at other deep-sea sites: Station M in the northeast Pacific Ocean (K. L. Smith et al. 1993, Kaufmann & Smith 1997) and the Porcupine Abyssal Plain in the northeast Atlantic Ocean (Bett et al. 2001) as well as in the lower estuary and Gulf of St. Lawrence (Belley et al. 2010). In addition to cameras that view the seafloor surface, sediment profile imaging systems inserted directly into the sediment provide supplementary information. They allow for the direct observation of burrowing behaviour as well as the vertical movement of luminophores (Solan et al. 2004).

Recently, 2 cabled seafloor observatories, VENUS (Victoria Experimental Network Under the Sea) in 2006, and NEPTUNE Canada (NorthEast Pacific Time-Series Undersea Networked Experiments) in 2009, have been deployed off the west coast of Canada. As these new technologies come into use, there is a need for new methodological approaches and observational protocols. This will ensure productive use of online observatory cameras and accompanying instruments for ecological studies. Acquiring continuous video streams is operationally simple, but impractically large quantities of data would need to be stored and processed. Although significant advances are being made in automated image analysis (Walther et al. 2004, Aguzzi et al. 2009, Purser et al. 2009) there are few, if any, software tools that can be reliably employed for *in situ* benthic studies. Most analyses still require labour-intensive manual processing of imagery by trained observers. In many cases, the amount of time required to process imagery surpasses the real-time duration of the footage. This severely limits the use of extensive video or photo records for ecological studies (Solan et al. 2003). In the deep sea where sunlight never penetrates, additional considerations related to light pollution from artificial sources must also be taken into account. The prolonged presence of unnatural lighting has the potential to negatively affect light-sensitive organs (Herring et al. 1999), influence the behaviour of the animals under study (Widder et al. 2005, Raymond & Widder 2007) and accelerate biofouling of instruments.

The greatest advantage of cabled observatory cameras for observational studies lies in their real-time and interactive capabilities. Their sampling frequency does not need to be determined before deployment. It can be refined based upon incrementally improving knowledge of the system or triggered in response to an unpredicted event (Delaney et al. 2000, Service 2007, Sherman & Smith 2009). Remotely controlled pan and tilt mechanisms afford a larger field of view (FOV) and allow for precise positioning and repositioning of the camera to study small features such as inhabited burrows. *In situ* observations of key benthic organisms in real-time can then be related to data on physical and chemical properties measured by nearby sensors (Sherman & Smith 2009).

This paper describes the development of an observation-to-modeling methodology for the quantitative study of surficial sediment bioturbation by megafauna at a NEPTUNE Canada cabled observatory site on the upper continental slope in the northeast Pacific Ocean, off Vancouver Island, British Columbia, Canada. We present the newly deployed observatory camera system, explain the observational protocol and provide a first estimate of megafaunal sediment-surface reworking rates (the time required to track over the entirety of the observed surface area) and their contribution to D_b at this site. Techniques for extracting quantitative information from the imagery acquired during the first year of deployment are described, as is the development of a Bayesian model. Bayesian inference is particularly well suited to research undergoing methodological optimization because previous

knowledge (acquired as methods are refined) can be incorporated in prior distributions of model parameters (Ellison 1996, 2004). A quantitative model of sediment-surface reworking rates can be created and improved upon as additional observations are made.

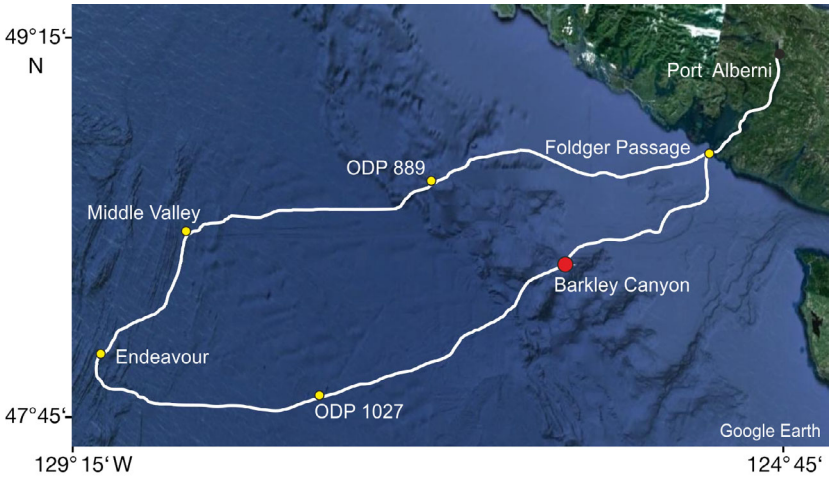

Fig. 1. NEPTUNE Canada's fibre optic backbone cable (white line) and node sites (circles) deployed on the west coast of Vancouver Island, British Columbia, Canada. The shore station is located in Port Alberni while the operation center is at the University of Victoria. The camera used in this study was deployed at the Barkley Canyon site, at a depth of 396 m

MATERIALS AND METHODS

Study area

Barkley Canyon, located 100 km off the coast of Vancouver Island, is a submarine canyon connecting the continental margin to the abyssal plain. This location was chosen for one of the regional nodes of the NEPTUNE Canada cabled observatory because of its suitability for the study of bentho-pelagic coupling as well as nutrient and sediment fluxes across the continental slope (Barnes et al. 2007). In 2009, the Barkley Canyon node was connected to the backbone fibre optic cable, allowing for real-time data to stream back to a shore station located in Port Alberni, British Columbia, and the operations centre at the University of Victoria (Fig. 1). An instrument platform (IP) with a black-and-white video camera was deployed near the canyon on the shelf-break (396 m depth, 48° 25′ 37.2″ N, 126° 10′ 29.7″ W).

Instruments and samples

The video camera used for this study was a low-light, black-and-white Multi-SeaCam® from Deep-Sea Power & Light. With a depth of field in water of 57° horizontal and 45° vertical, it yielded a surface of observation of ~0.9 m^2 per frame. The camera was mounted on a remotely controlled pan and tilt mechanism whose physical limitations reduced camera rotation to less than a full 360°, creating a blind spot near the rear left leg of the platform that accounted for 30% of the FOV. The total FOV was evaluated as having a radius of 200 cm, for a total of 8.8 m^2. The camera control web interface allowed for semi-automated observations by using predetermined camera positions. The camera was also equipped with 2 parallel 635 nm laser beams positioned 10 cm apart and used for image scaling. In addition, the lighting system was composed of a pair of ROS SmartLIGHT II lamps equipped with 7 adjustable LED lights (5500K, 570 lx at 1 m) positioned 24 cm on either side of the lens. The remotely operated vehicle (ROV) ROPOS (operated by the Canadian Scientific Submersible Facility) deployed a 2 m long, white PVC pipe marked at 10 cm intervals to act as a scaling ruler. The pipe was laid on the seafloor perpendicular to the long axis of the IP, with one end directly below the camera on the seafloor (Nadir point) and the other extending away from the study area. The recorded video streams were stored by NEPTUNE Canada's data archiving system DMAS. These archived videos can be downloaded online using the Oceans 2.0 Toolbox (registration required, www.neptunecanada.ca/data-collaboration/). Live video streams can also be viewed online at www.neptunecanada.ca/news/live-video/current-video-streams.dot.

To characterize decimetre-scale changes in the surficial sediment surface, images from a Kongsberg Mesotech Rotary sonar with 1071 heads deployed on the IP were also examined. This instrument collected images at 675 kHz, which were then analyzed for the formation and turnover rates of sediment surface structures. Bottom current velocities were assessed with a 600 kHz acoustic Doppler current profiler (ADCP) (RDI Workhorse Monitor, RD Instruments) also located on the IP. Two push cores were taken next to the IP using the ROV, preserved in buffered 10% formalin and analyzed for grain size. A laser diffraction particle size analyzer (LS 13320, Beckman-

Coulter) was used for fine sediments (<2 mm), while larger sediments (≥2 mm) were dried at 60°C for 48 h and sieved (0.25 phi precision).

Observation regime

As a precaution against potential negative effects of light pollution, lighting was limited to 1 h d^{-1}, but could be allocated as desired throughout the day. Three different observation regimes were tested to determine the most appropriate one to quantify rates of sediment-surface reworking by the megafaunal community at this site. These consisted of 1 continuous hour (from 4 January to 25 February 2010), two 30 min periods (from 24 March to 9 April 2010) and 5 min every second hour (15 April to 12 June and 25 August to 23 October 2010).

The hour-long observations were used as an introduction to the system and allowed us to establish that sea urchins and flatfishes represented the major megafaunal contributors to surface bioturbation (see 'Results'). From there, we focused on quantifying their size, abundance and movement patterns. The residence time of flatfish within the FOV was less than 60 min, but this sampling duration did not permit detection of displacement by sea urchins. Doubling the sampling frequency (2 × 30 min d^{-1}) allowed us to observe more individual sea urchins, but was insufficient to describe their movement patterns because individuals usually stayed less than 12 h within the FOV. We therefore elected to increase the sampling frequency while respecting the daily lighting time limit. A minimum of 5 min was required for the camera to cover the entire FOV. Twelve 5 min observation periods per day was therefore the maximal frequency attainable without losing the increased FOV afforded by the pan and tilt mechanism. This regime allowed for movement tracking, increased overall flatfish sightings and collected a quantity of information that could still be managed by a single observer.

In addition to the daily lighting limit, supplementary short bursts of interactive image sampling at increased rates could be implemented in response to specific events such as phytoplankton blooms in the upper water column. When cloud cover did not interfere, phytoplankton blooms could be detected in near real-time by consulting maps of chlorophyll *a* (chl *a*) concentration produced by OceanColor (http://oceancolor.gsfc.nasa.gov/) from data collected by the NASA satellite MODIS AQUA. Data from the SeaWiFs satellite, obtained through NASA's web-based GIOVANNI application developed by GES DISC (http://disc.sci.gsfc.nasa.gov/giovanni), were used to define historical trends in surface chl *a* concentrations for this location.

Construction of perspective grids

Perspective grids were constructed to measure objects in the oblique images, based on the method of Wakefield & Genin (1987). We made *in situ* optical measurements to compensate for any sinking of the camera platform legs into the sediment after deployment. Perspective grids were built by using the paired lasers mounted on the camera, and the perpendicular scaling ruler was placed on the seafloor within the FOV. The distance between the laser beams varied predictably with the tilt position of the camera and could be used to trace the meridian lines of the perspective grid. Horizontal lines for the perspective grid were drawn based on the vertical scale obtained by using the position of the scaling ruler's 10 cm increments (Fig. 2). Because the IP changed locations after the maintenance cruise in May 2010 (leading to variations in the depth to which the legs sank into the soft sediment), separate grids were built for each deployment. The image analysis freeware ImageJ (http://rsbweb.nih.gov/ij/) developed by the National Institutes of Health, USA, was employed for perspective grid construction and subsequent measurements.

The perspective grids were overlaid on extracted video frames to measure animal size and displace-

Fig. 2. Example of a perspective grid. The scaling ruler with 10 cm increments is visible in the center of the image (white PVC pipe) and the laser beams are also separated by 10 cm. Hence, each square represents 100 cm^2 on the seafloor for a surface of ~0.9 m^2 per frame

ment. K. L. Smith et al. (1993) used perspective grids to follow the movement of organisms from one observation period to the next. In our case, to accommodate the circular study area, a polar coordinate system based on readings from the pan and tilt mechanism was developed. Organism positions could then be described based on their distance from a fixed point and its azimuth (angle away from a reference direction). Here, the fixed point was the Nadir point and the reference direction was considered to be a pan value of zero. The position of each individual was recorded and plotted over time on a circular map representing the FOV. The Euclidean distance between 2 subsequent positions was used as an estimate of the minimum distance travelled by the individual. More detailed descriptions of the methodology employed are provided in Robert (2011).

Sea urchin and flatfish sediment-surface reworking rates

Imprints caused by the disturbance and displacement of sediment by the 2 megafaunal organisms monitored could not be resolved by using the present camera system; hence, animal dimensions and movement patterns were used to obtain an estimate of the time required to completely track over the surficial sediment (sediment-surface reworking rates) observed in the FOV. The model parameters used were similar to those described in Lohrer et al. (2005) except that our model utilized a Bayesian approach. Distributions for animal imprint areas on the sediment, movement rates and abundances were compiled. In the case of sea urchins, animal width and minimal distance travelled between sightings were used to determine the surface area tracked in $cm^2\ h^{-1}$ (Kaufmann & Smith 1997). Abundances were compiled per residence period, 8 h for sea urchins and 1 h for flatfish, in order to minimize sampling of organisms more than once.

Bayesian model

Bayesian inference is based on Bayes' theorem (Bayes 1763):

$$P(\theta|Y) = \frac{f(Y|\theta)P(\theta)}{P(Y)} \quad (1)$$

where $P(\theta|Y)$ represents the 'posterior' or probability of obtaining the parameter θ given the data Y, $P(\theta)$ is the 'prior' containing previous information regarding the hypothesis, $f(Y|\theta)$ is the 'likelihood' function, and $P(Y)$ is a normalizing constant. This constant cancels out when Markov chain Monte Carlo (MCMC) methods are used to estimate the form of the posterior distribution (Gelman et al. 1995, Ellison 1996). For the first iteration of the model presented in this study, 'uninformative priors' were used. However, with this modeling approach it will be easier to refine subsequent estimates, by updating priors as new data are acquired over the lifetime of the observatory by other experimenters.

Because the equation representing the posterior distribution cannot always be easily calculated, its form and statistical properties are estimated by using MCMC methods. Thousands of iterations are performed, eventually forming a chain of values. Multiple chains are created and their values will converge to the form the posterior distribution. Initial values are discarded to minimize the influence of the starting point of each chain, and thinning of individual chains is carried out to reduce possible occurrence of correlations between values (refer to McCarthy 2007 for a comprehensive view of Bayesian methods for ecologists). By using the freeware WinBUGS (www.mrc-bsu.cam.ac.uk/bugs/), 3 chains, whose initial 1000 iterations were discarded and where only 1 out of 3 iterations was retained, were used to ascertain convergence. This resulted in 10 000 iterations from which posterior distributions were calculated. As the sea urchin width and movement rate and the flatfish area data were close to normal, they were modeled using normal distributions. The use of a bivariate normal distribution for the area reworked by sea urchins allowed missing movement rates to be internally computed within WinBUGS, based on sea urchin width and the covariance function. As abundances can only be positive integers, they were modeled by using a Poisson distribution; a log normal prior was used to help with overdispersion in the data.

Using the statistical package R (www.r-project.org/), a random draw was made (one for the sea urchins and one for the flatfish) from the posterior distributions of organism abundance (n) per residence period. For flatfish, n draws were generated from the distributions of area reworked. For sea urchins, the area reworked was obtained by drawing a width value and multiplying it by a movement rate value. This was repeated n times. The previous steps were repeated in order to scale up to 24 h (residence period of 8 h for sea urchins and 1 h for flatfish). The total area disturbed was summed, and a new value was calculated each day. Based on these daily simulations, the number of days required to track over the

entire area represented in the FOV (8.8 m^2) was computed for both sea urchins and flatfish. This entire process was repeated 500 times to determine the variability in our estimate and account for the uncertainty associated with having used a small sample size to estimate parameters. A schematic illustrating the steps taken is provided in Fig. 3.

Biodiffusion coefficient

The modeled sediment-surface reworking rates (representing only mechanical mixing, not changes in sediment composition following ingestion) were investigated further by calculating the contribution of the megafauna to D_b at this site. At the microscopic level, particle movement (vertical or horizontal) can be modeled using a random walk described by a distance travelled ('jump length' distribution) and a waiting time until the next jump event ('waiting time' distribution) (refer to Meysman et al. 2008a,b for derivations and model validation). From these 2 distributions, D_b can be calculated with the formula:

$$D_b = \frac{\sigma^2}{2\tau_c} \quad (2)$$

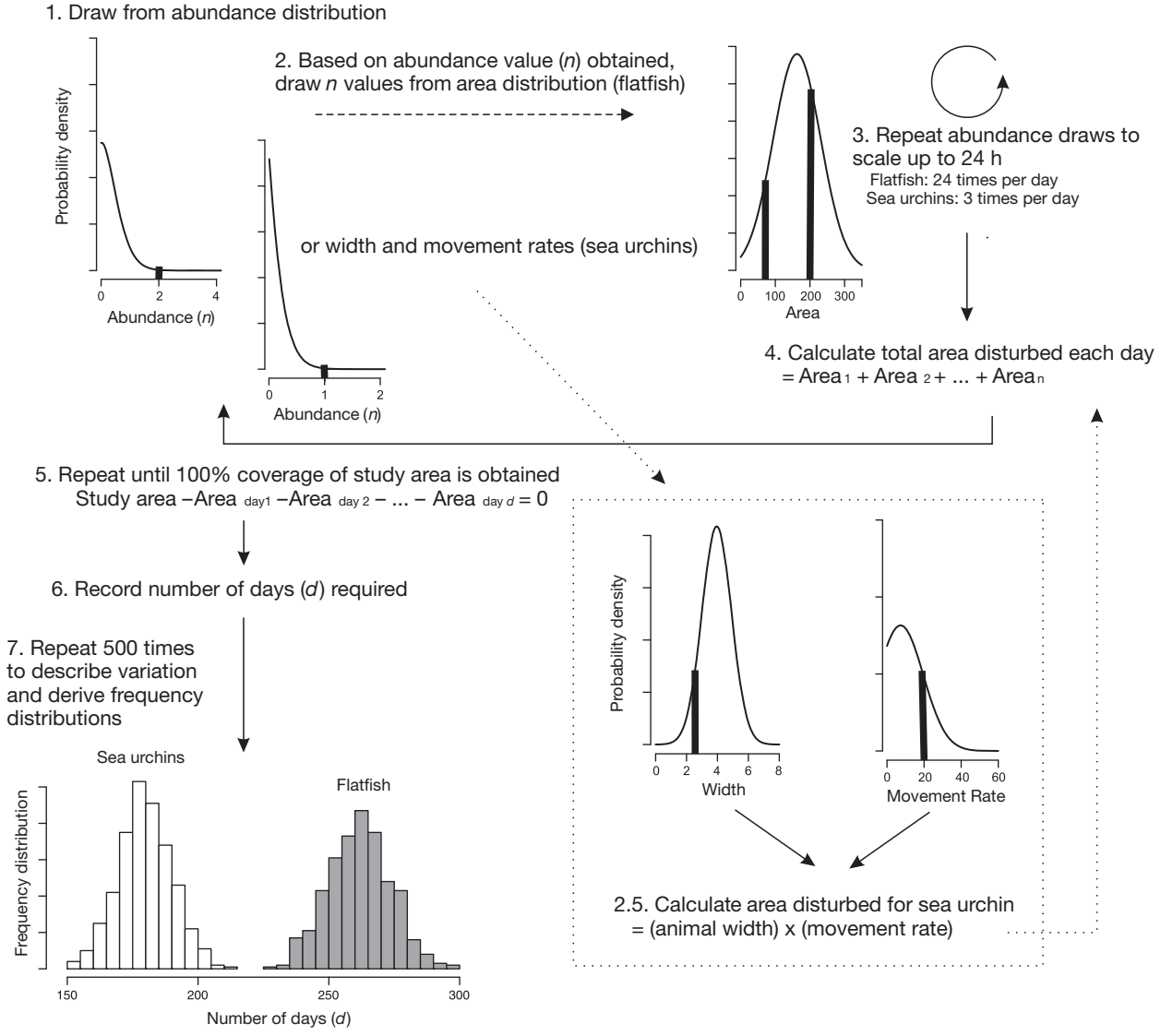

Fig. 3. Schematic representation of the steps taken to obtain estimates of the number of days required to fully track over the study area by using probability density functions estimated in WindBUGS based on the raw data extracted from the imagery of surficial sediment disturbances by flatfish and sea urchins (data shown in Fig. 5). The depicted steps were carried out within the statistical package R

where σ is the SD of the jump length distribution and τ_c is the mean of the waiting time distribution. The mean waiting time was obtained from the estimated number of days required for the megafaunal community to turn over the FOV (Wheatcroft et al. 1990). Very little information is available regarding the jump length of a particle displaced by a sea urchin or a flatfish. As such, the jump length distributions are only described very coarsely based on likely maximal displacement length of a particle resulting from a single bioturbation event and the expectation that small jump lengths would occur more frequent than long ones. For flatfish the upper distribution limit represented the average radius of a flatfish (horizontal direction, x) and a depth of 1.0 cm (vertical direction, y). In the case of sea urchins, maximal horizontal displacement was set at half the average width of an organism. As they cause very little sediment subduction, the maximal vertical displacement would be minimal and was set at 0.30 cm. From the given likely spread of jump length values, very coarse SD values could be defined, but the actual shape of the distribution remains unknown. The calculated $D_{b(x,y)}$ only represent coarse estimates of the contribution of sea urchins and flatfish to horizontal and vertical sediment mixing at this site.

RESULTS

The most commonly observed megafauna consisted of rockfish *Sebastes* sp., flatfishes (Dover sole *Microstomus pacificus* and Pacific halibut *Hippoglossus stenolepis*), skates (longnose skate *Raja rhina* and skates *Bathyraja* spp.), fragile pink sea urchin *Allocentrotus fragilis*, snails (family: Buccinidae) and an orange anemone (order: Actiniaria). Of these organisms, only flatfish, sea urchins and buccinid snails were commonly observed disturbing the sediment surface. However, snail locomotion rates and abundances could not be accurately resolved within the 60 min d^{-1} lighting-time observation regime. No phytodetrital accumulations were observed in the FOV of the camera, and in contrast with the previous decade, no pronounced phytoplankton bloom was recorded in the satellite imagery of the waters overlying Barkley Canyon in the spring of 2010 (data not shown).

The rotary sonar recorded abundant, ~40 cm diameter pits surrounding the IP, whose location did not change in 6 mo (A. E. Hay pers. obs.). These pits were also observed during ROV surveys over a larger area (~1 km^2) of shelf-break near Barkley Canyon (K. Robert pers. obs.). The centers of the pits were visually estimated to be 7 to 10 cm lower than the sediment surface at their outer edges. Grain size analysis of the 2 push cores showed that the upper 2 cm of sediment were respectively composed of 2.3 and 7.2% clay, 11.6 and 33.3% silt, 36.1 and 34.5% very fine sand, and 48.49 and 20.4% fine sand (Fig. 4). Based on grain size and analysis of current velocities, the Shields parameter indicated that bottom stress was very rarely high enough for bottom currents to resuspend the sediments and thereby cause the formation of these pits (A. E. Hay pers. obs.).

In total, 99 sea urchins and 49 flatfish were used to obtain posterior distributions of the sediment area reworked. Sea urchins had a mean (±SD) width of 3.95 ± 0.96 cm and an average speed of 7.31 ± 12.23 cm h^{-1} (Fig. 5a,b), which resulted in an area of sediment displaced at a rate of 33.9 ± 6.79 cm^2 h^{-1}. The imprints left in the sediment by flatfish averaged 162.5 ± 68.81 cm^2 (Fig. 5d). More than 150 h of video footage were collected and yielded posterior distributions for abundance that predicted 1.7 sea urchins and 2.1 flatfish were likely to cross the FOV on a daily basis (Fig. 5c,e). However, flatfish abundance was likely underestimated as a result of their short residence time (<60 min) within the FOV. Our model predicted that sea urchins have the ability to completely track the surface of the 8.8 m^2 FOV within 153 to 213 d while the contribution by flatfish would be slightly slower, ranging from 227 to 294 d (Fig. 6). This represents sediment-surface reworking rates of 26.0 to 35.1 m^2 yr^{-1} for this site (flatfish: 10.9 to 14.1 m^2 yr^{-1}, sea urchins:

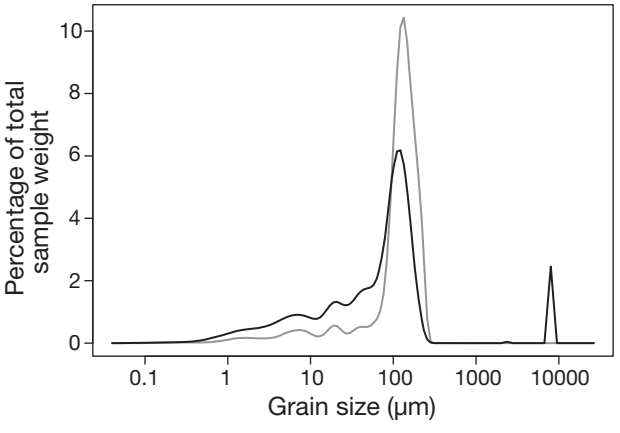

Fig. 4. Grain size distribution of the upper 2 cm of sediment based on percentage of sample weight for 2 push cores taken in proximity to the instrument platform (Push-core 1: grey, Push-core 2: black)

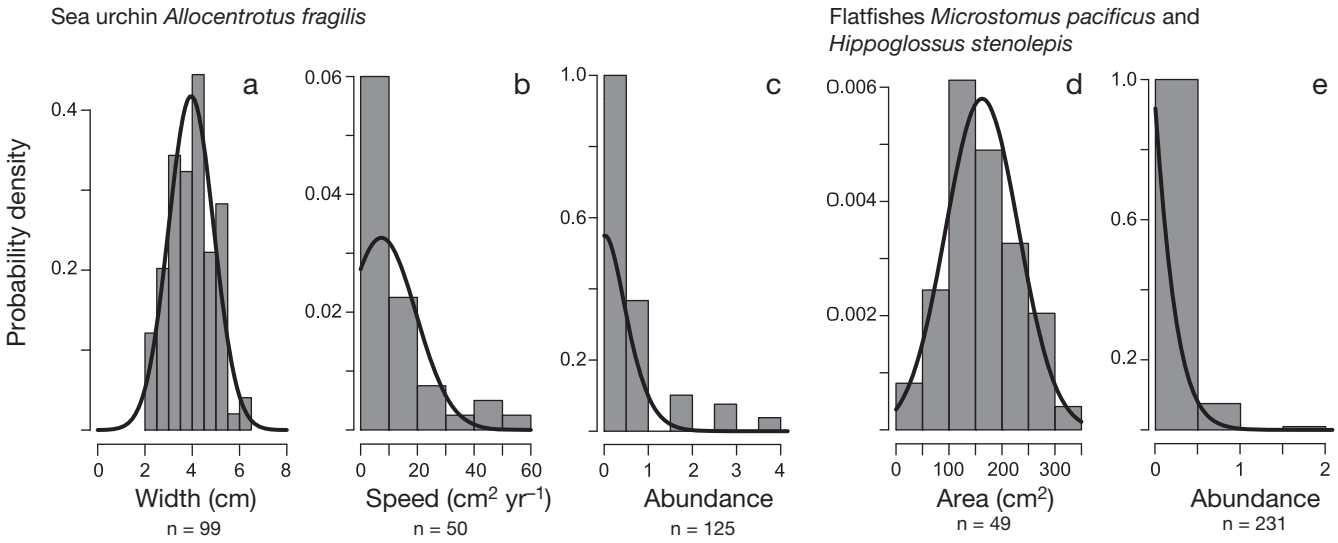

Fig. 5. Posterior probability distributions overlaid on the histogram of the measured variables for the 2 megafaunal surface bioturbator taxa. Abundances were compiled per residence period, 8 h for sea urchins and 1 h for flatfish

15.1 to 21.0 m^2 yr^{-1}), which roughly translates into a mean waiting time of 0.25 to 0.34 yr (flatfish: 0.62 to 0.81 yr, sea urchins: 0.42 to 0.58 yr). The SDs for the flatfish jump length distributions were set at 2.0 cm for the horizontal direction (giving maximal values approximating mean flatfish radius, 7.02 cm) and 0.30 cm in the vertical direction, while for sea urchins it was set as 0.58 cm (horizontal direction) and 0.09 cm (vertical direction). For flatfish, this represents estimates of 2.5 to 3.2 cm^2 yr^{-1} for $D_{b(x)}$ and 0.056 to 0.073 cm^2 yr^{-1} for $D_{b(y)}$, while estimates of 0.29 to 0.40 cm^2 yr^{-1} for $D_{b(x)}$ and 0.006 to 0.009 cm^2 yr^{-1} for $D_{b(y)}$ were obtained for sea urchins.

DISCUSSION

Sediment-surface reworking rates and biodiffusion coefficients

Although extrapolations based on small data sets need to be viewed carefully, the estimated 26.0 to 35.1 m^2 yr^{-1} sediment-surface reworking rates were not inconsistent with values reported in the literature. At Station M at 4100 m depth in the northeast Pacific Ocean, estimates of sediment-surface reworking rates ranged from 36.0 m^2 yr^{-1} (Kaufmann & Smith 1997) to 70.4 m^2 yr^{-1} (K. L. Smith et al. 1993). Turnover rates were lower at 4850 m in depth at the Porcupine Plain of the northeast Atlantic Ocean, where values ranged from 0.6 to 2.6 m^2 yr^{-1} (1991–1994) to 11.6 to 29.7 m^2 yr^{-1} (1997–2000) (Bett et al. 2001).

For both flatfish and sea urchins together, we estimated $D_{b(y)}$ values of 0.062 to 0.082 cm^2 yr^{-1} and $D_{b(x)}$ values of 2.8 to 3.6 cm^2 yr^{-1}. Tracer-derived D_b from the Porcupine Plain ranged from 0.14 to 1.26 cm^2 yr^{-1} (^{210}Pb) (Carvalho et al. 2011), while values ranging from 0.3 to 0.6 cm^2 yr^{-1} (^{210}Pb) and 7.9 to 200 cm^2 yr^{-1} (^{234}Th) were measured at a shallower California site

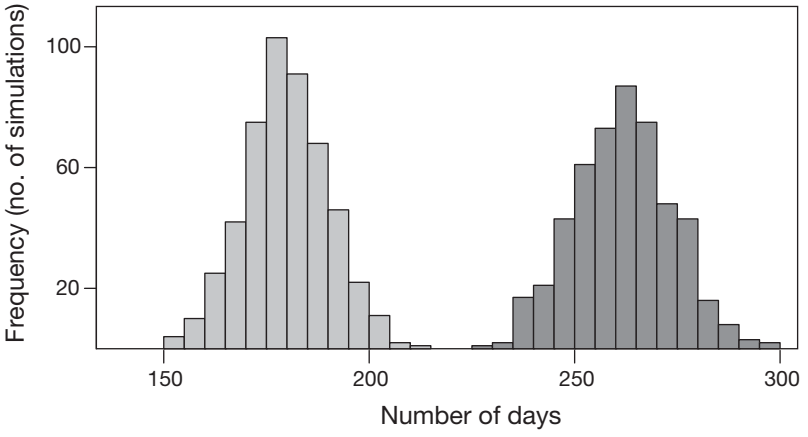

Fig. 6. Frequency distribution based on 500 simulations showing the expected number of days required for 2 megafaunal surface bioturbator taxa (the flatfishes *Microstomus pacificus* and *Hippoglossus stenolepis* in dark gray, and the sea urchin *Allocentrotus fragilis* in light gray) to fully rework the surficial sediments within the 8.8 m^2 of the study area

(1240 m). Along the continental slope (200 to 3000 m in depth) median D_b values obtained through global analysis indicated similar rates: 0.57 cm^2 yr^{-1} (^{210}Pb) and 10 cm^2 yr^{-1} (^{234}Th) (Lecroart et al. 2010). The biodiffusion model has been demonstrated to only hold when a very large number of mixing events have taken place and when the time between mixing events is extremely short (Meysman et al. 2010). Although the length of time required to satisfy this assumption depends on the particle mixing rate, it usually remains too short when using tracers such as ^{234}Th and results in larger D_b estimates (Reed et al. 2006). Estimates for particle-derived D_b have also been obtained by using the lattice-automaton bioturbation simulator (LABS), a virtual sediment particle environment where individual particles were tracked to assemble waiting time and jump length distributions (Reed et al. 2006). Based on the slope environment simulation, step length and waiting time of 0.13 cm and 0.044 yr, respectively, were estimated, which yielded a D_b value of 0.19 cm^2 yr^{-1} (Lecroart et al. 2010). As only 2 megafaunal groups were considered in this study, our smaller $D_{b(y)}$ values are to be expected because we are currently unable to measure infaunal contributions with this seafloor camera system. *In situ* estimates and experimentations at other sites will be needed to better characterize waiting time and jump length distributions in slope environments. Wheatcroft (1991) previously noted that horizontal surface mixing of sediment may be occurring at much faster rates than those recorded using tracer profiles of sediment. Few current geochemical models consider the role of horizontal mixing in the decomposition of newly sedimented organic matter. Differences in seafloor morphology, depth, organic matter fluxes and species assemblages between all these studies limit the value of further comparisons.

Additional data being collected from 2 other NEPTUNE Canada IPs located farther down Barkley Canyon will generate a more thorough description of the spatial variation (across shelf-break depth gradients) in bioturbation levels, particularly with respect to depth and topographic features. The use of multiple sites within the same region will also provide a better appreciation of the spatial scale to which bioturbation levels can be extrapolated. Evidence from other submarine canyon systems suggests that for a given depth, bioturbation rates within canyons are higher compared to other slope environments, and that within an individual canyon, higher bioturbation rates are found in its upper sections (De Leo et al. 2010, García et al. 2010).

Bioturbation at the shelf-break

Echinoderms often dominate deep-sea habitats and have been given much consideration in discussions of bioturbation. The fragile pink sea urchin, the most common echinoderm observed in our FOV, probably influences sediment organic matter content when feeding on phytodetritus (Giese 1961), but no obvious trails or burrowing behaviours have been reported for this species. Their contribution to particle mixing is probably limited to horizontal transport of the upper surface with very little subduction. This species is known to form high density aggregations (Boolootian et al. 1959); in such cases their contribution to bioturbation will exhibit high spatial variability at scales greater than the patch size. No such aggregations were observed with the NEPTUNE Canada camera, but some were observed during general ROV maintenance surveys in the general area (K. Robert pers. obs.). The overall slow locomotion of sea urchins resulted in a limited ability to accurately quantify movement rates with the longer, less frequent observation regimes. By making 5 min observations every 2 h, we were able to estimate their movement rates and the likelihood of an individual going undetected was reduced. The movement rates determined for *Allocentrotus fragilis* (average: 7.31 cm h^{-1}, maximum: 324.8 cm h^{-1}) were consistent with laboratory observations by Salazar (1970). The fastest speeds were recorded during the longer observation periods and represented only short rapid bursts of movement instead of sustained locomotion speeds. Salazar (1970) found *A. fragilis* to exhibit maximal speed during illumination periods, emphasizing the need to limit artificial light exposure in deep-sea studies. In this initial model, individual sea urchins were assumed to move randomly at a constant speed across the FOV for an average residence time of 8 h. This approach is oversimplified as it does not account for crossing over of freshly tracked sediment, and the constant speed assumption is inconsistent with what is known of the foraging behaviour of echinoderms (Dusenbery 1989). As more information on movement patterns becomes available, calculating the actual area tracked by individual animals will provide a more accurate model.

The regime of a 5 min observation every 2 h also increased the number of flatfish observed, but an even higher sampling frequency would be advantageous for these fish. The addition of high frequency, fixed-position snapshots of a section of the FOV would probably improve the accuracy of abundance estimates without considerably increasing lighting

time. Although, none of the flatfish species encountered appeared to respond to the artificial lighting used during the observations, at another site located deeper within the canyon at 891 m, sablefish (black cod) *Anoplopoma fimbria* commonly swam toward the camera when the video lights were turned on (K. Robert pers. obs.). There was even a point during the course of the observation period when increasing densities of these fish impaired the monitoring of the benthic fauna. There are few *in situ* studies of the responses of deep-water organisms to artificial lighting (Widder et al. 2005, Raymond & Widder 2007).

The depressions recorded by the sonar around the shelf-break IP could originate and be maintained through micro-scale habitat selection by flatfish. Both Dover sole and Pacific halibut were observed to bury themselves in the upper layer of sediment and leave shallow oval imprints (1 to 2 cm) upon departure. Similar sedimentary features created by small flatfish have been documented by Yahel et al. (2008) from a shallower soft sediment fjord (~100 m). Once created, these depressions could be reused regularly, either for protection against predators or enhanced prey capture (Auster et al. 1995). This could explain the deeper pit depths we observed, the very rare observation of new pit formation and possibly their persistence over time. However, low bottom stress would also significantly delay infilling (A. E. Hay pers. obs). Behavioural studies of flatfishes have already found them to significantly associate with sediment structures, such as sand waves, and depressions produced by other species (Norcross & Mueter 1999, Busby et al. 2005, Stoner et al. 2007). This behaviour was also observed during ROV operations carried out around the shelf-break site (K. Robert pers. obs.). Our modeled results suggested that flatfish reworked the entire study area in a matter of months. If instead their activity was focused in depressions, these would be visited on a more frequent basis. This implies that sediment-surface reworking rates may vary substantially over ~10 cm spatial scales within the FOV. The co-located rotary sonar, which allows for observation of a greater surface area at higher sampling rates, will now be employed to determine how frequently these pits may be visited by flatfish.

Rays are also known as major bioturbators in certain coastal systems and can leave oval imprints 6 to 10 cm deep in the sediment (Howard et al. 1977, Gregory et al. 1979, Thrush et al. 1991, Martinell et al. 2001). Although we could not find any reference in the literature to imprint formation in the observed skate species, and this behaviour was not recorded by our cameras, bottom feeding by skates could also explain the sedimentary features observed by the rotary sonar and ROV. Formation of a similar-sized depression has been reported for the little skate *Raja erinacea* (Auster et al. 1995). However, if only this process was at work, sediment infilling would eventually occur. The pits observed in this study remained for 6 mo (A. E. Hay pers obs), which contrasts with the shorter existence times of other smaller biogenic sedimentary features, such as openings of abandoned burrows and buccinid trails (K. Robert pers. obs.).

System improvement and future use

In addition to improved camera systems and programmable image acquisition, automated object detection software will be essential for processing large-image data sets in order to reduce the bottleneck caused by our present reliance on manual annotations. Software is available for automated detection of events and objects in the water column (Walther et al. 2003); however, for seafloor imagery, the increased complexity of the background as well as the partial occlusion and high density of organisms have slowed the implementation of automated object detection algorithms in benthic studies. Progress has been made using neuromorphic vision algorithms (Cline et al. 2008), local invariant features (Gobi 2010), Fourier descriptors (Aguzzi et al. 2009), Canny edge detection and Delaunay triangulation (Taylor et al. 2008). However, for the present, manual processing remains the most accurate method for analysis of complex benthic imagery.

The present study provides one approach to optimizing data collection and extraction of ecologically meaningful information that is extendable to other camera systems and locations. As an initial step with a new system, a single, continuous observation period is appropriate for gaining familiarity with the operating system as well as for determining the composition and behaviour of the community present in the FOV. Once the community is characterized, the parameters needed to quantify the process of interest need to be identified. The observation frequency can then be increased incrementally until changes are perceived. Higher frequencies that provide more accurate estimates can be implemented until the time required for data processing becomes impractical for long-term monitoring or technical limitations are reached. Each parameter will vary in its range of effective observation frequencies, and

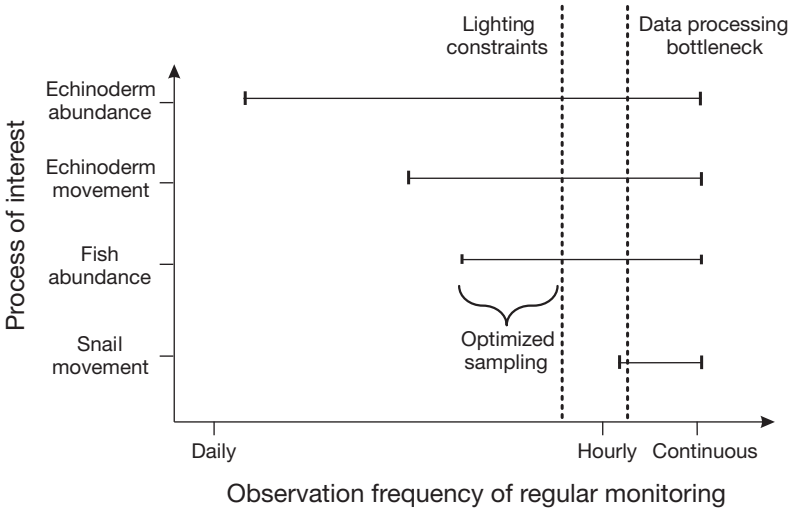

Fig. 7. Schematic representation of the sampling protocol challenges for long-term regular monitoring. The goal is to find a sampling frequency that will maximize the information gathered for several processes occurring at various temporal scales while ensuring that logistical constrains such as lighting-time allocation (left dashed line) are not exceeded and that data processing remains feasible (right dashed line)

areas of overlap represent optimal observation frequencies for several processes of interest. A schematic representation of this approach as exemplified by bioturbation processes observed in this study is provided in Fig. 7.

Once a data set is built, parameters can be estimated and the processes of interest can be modeled. Significant differences in the philosophical underpinnings of Bayesian and frequentist approaches to inference and hypothesis testing exist (e.g. Bayesian inference conditions probability statements on the observed data, instead of estimating the probability of obtaining the data given the null hypothesis) and their respective advantages continue to be discussed in the literature (Dennis 1996, Ellison 2004, Stephens et al. 2007). In our study, the ability to incorporate our initial estimates, collected while resolving the observation schedule, into longer-term studies to be carried on the NEPTUNE Canada cabled observatory and the ease with which missing data could be handled (Gelman et al. 1995) were the main reasons for choosing a Bayesian approach. Hierarchical designs that include additional species, seasonal trends in response to organic matter sedimentation or spatial variation based on depth can also be included in the model once supplementary environmental data have been collected. Comparisons between studies will also be enhanced by the application of standardized observation protocols.

CONCLUSION

Long-term monitoring by means of seafloor observatories will provide valuable insights into the response of seafloor ecosystems to changes in primary productivity and related organic matter supply (Smith et al. 2009, Larkin et al. 2010). Changes in upper water primary productivity will propagate to the benthos, which is already food-limited (Smith & Kaufmann 1999). In megabenthic species, quick behavioural responses (Kaufmann & Smith 1997, Grémare et al. 2004, Vardaro et al. 2009) as well as changes in species composition and biomass (Billett et al. 2001, 2010, Ruhl & Smith 2004) are to be expected. As a result, bioturbation and other ecosystem services in the deep sea are also likely to be affected. Baseline characterization of the current state of this biome is essential for future quantitative evaluation of the impacts of global climate change and increased anthropogenic disturbance on ecosystem processes. Bioturbation is an important ecological service influenced by a variety of environmental factors whose characterization in the deep sea requires an integrated approach well suited to cabled observatories as exemplified in this study.

Acknowledgements. We thank Dr. M. Best and NEPTUNE Canada for the at-sea opportunities as well as the support provided for the use of the camera system. Thanks go to the ROPOS team for all the good work installing the various pieces of equipment. Also, special thanks go to J. William, K. Wallace and N. Scott for all the trouble-shooting regarding the cameras, Dr. A. Hay and D. Schillinger for access to the rotary sonar data, Dr. P. Archambault for the grain size analysis and Dr. F. Nathoo for the help with Bayesian analyses. This research was supported by the Natural Sciences and Engineering Research Council of Canada through a Discovery grant to S.K.J. and a Strategic Networks grant to the Canadian Healthy Oceans Network.

LITERATURE CITED

Aguzzi J, Costa C, Fujiwara Y, Iwase R, Ramirez-Llorda E, Menesatti P (2009) A novel morphometry-based protocol of automated video-image analysis for species recognition and activity rhythms monitoring in deep-sea fauna. Sensors 9:8438–8455

Aller RC (1982) The effect of macrobenthos on chemical properties of marine sediment and overlying water. In: McCall PL, Tevesz MJS (eds) Animal–sediment relations. Plenum Press, New York, NY, p 53–102

Auster P, Malatesta R, LaRosa S (1995) Patterns of microhabitat utilization by mobile megafauna on the southern New England (USA) continental shelf and slope. Mar Ecol Prog Ser 127:77–85

Barnes CR, Best MMR, Bornhold BD, Juniper SK, Pirenne B, Phibbs P (2007) The NEPTUNE project — a cabled ocean observatory in the NE Pacific: overview, challenges and scientific objectives for the installation and operation of Stage I in Canadian waters. In: Symposium on underwater technology and workshop on scientific use of submarine cables and related technologies, 17–20 April 2007, Tokyo, p 308–313

Bayes T (1763) An essay towards solving a problem in the doctrine of chances. Philos Trans R Soc Lond 53:370–418

Belley R, Archambault P, Sundby B, Gilbert F, Gagnon JM (2010) Effects of hypoxia on benthic macrofauna and bioturbation in the Estuary and Gulf of St. Lawrence, Canada. Cont Shelf Res 30:1302–1313

Bett BJ, Malzone MG, Narayanaswamy BE, Wigham BD (2001) Temporal variability in phytodetritus and megabenthic activity at the seabed in the deep Northeast Atlantic. Prog Oceanogr 50:349–368

Billett DSM, Bett BJ, Rice AL, Thurston MH, Galéron J, Sibuet M, Wolff GA (2001) Long-term change in the megabenthos of the Porcupine Abyssal Plain (NE Atlantic). Prog Oceanogr 50:325–348

Billett DSM, Bett BJ, Reid WDK, Boorman B, Priede IG (2010) Long-term change in the abyssal NE Atlantic: the '*Amperima* Event' revisited. Deep-Sea Res II 57: 1406–1417

Booloottian RA, Giese AC, Tucker JS, Farmanfarmaian A (1959) A contribution to the biology of a deep sea echinoid, *Allocentrotus fragilis* (Jackson). Biol Bull (Woods Hole) 116:362–372

Bradshaw C, Kumblad L, Fagrell A (2006) The use of tracers to evaluate the importance of bioturbation in remobilising contaminants in Baltic sediments. Estuar Coast Shelf Sci 66:123–134

Busby MS, Mier KL, Brodeur RD (2005) Habitat associations of demersal fishes and crabs in the Pribilof Islands region of the Bering Sea. Fish Res 75:15–28

Carvalho FP, Oliveira JM, Soares AMM (2011) Sediment accumulation and bioturbation rates in the deep Northeast Atlantic determined by radiometric techniques. ICES J Mar Sci 68:427–435

Cline DE, Edgington DR, Mariette J (2008) An automated visual event detection system for cabled observatory video. In: 3rd Int Conf Computer Vision Theory Appl, 22–25 January 2008, Funchal, Madeira, p 22–28

De Leo FC, Smith CR, Rowden AA, Bowden DA, Clark MR (2010) Submarine canyons: hotspots of benthic biomass and productivity in the deep sea. Proc Biol Sci 277: 2783–2792

Delaney J, Heath GR, Chave A, Kirkham H and others (2000) NEPTUNE: real-time, long-term ocean and earth studies at the scale of a tectonic plate. Oceanography 13:71–79

Dennis B (1996) Discussion: Should ecologists become Bayesians? Ecol Appl 6:1095–1103

Dusenbery DB (1989) Ranging strategies. J Theor Biol 136: 309–316

Ellison AM (1996) An introduction to Bayesian inference for ecological research and environmental decision-making. Ecol Appl 6:1036–1046

Ellison AM (2004) Bayesian inference in ecology. Ecol Lett 7: 509–520

García R, Thomsen L, de Stigter HC, Epping E, Soetaert K, Koning E, de Jesus Mendes PA (2010) Sediment bioavailable organic matter, deposition rates and mixing intensity in the Setúbal-Lisbon canyon and adjacent slope (Western Iberian Margin). Deep-Sea Res I 57:1012–1026

Gelman A, Carlin J, Stern H, Rubin D (1995) Bayesian data analysis. Chapman & Hall, London

Gerino M, Aller RC, Lee C, Cochran JK, Aller JY, Green MA, Hirschberg D (1998) Comparison of different tracers and methods used to quantify bioturbation during a spring bloom: 234-thorium, luminophores and chlorophyll *a*. Estuar Coast Shelf Sci 46:531–547

Giese AC (1961) Further studies on *Allocentrotus fragilis*, a deep-sea echinoid. Biol Bull (Woods Hole) 121:141–150

Gobi AF (2010) Towards generalized benthic species recognition and quantification using computer vision. In: 4th Pacific-Rim Symposium on Image and Video Technology (PSIVT), 14–17 November 2010, Singapore, p 94–100

Gregory MR, Ballance PF, Gibson GW, Ayling AM (1979) On how some rays (Elasmobranchia) excavate feeding depressions by jetting water. J Sediment Res 49:1125–1129

Grémare A, Duchêne JC, Rosenberg R, David E, Desmalades M (2004) Feeding behaviour and functional response of *Abra ovata* and *A. nitida* compared by image analysis. Mar Ecol Prog Ser 267:195–208

Herring PJ, Gaten E, Shelton PMJ (1999) Are vent shrimps blinded by science? Nature 398:116

Howard JD, Mayou TV, Heard RW (1977) Biogenic sedimentary structures formed by rays. J Sediment Res 47: 339–346

Kaufmann RS, Smith KL (1997) Activity patterns of mobile epibenthic megafauna at an abyssal site in the eastern North Pacific: results from a 17-month time-lapse photographic study. Deep-Sea Res I 44:559–579

Lampitt RS, Bett BJ, Kiriakoulakis K, Popova EE, Ragueneau O, Vangriesheim A, Wolff GA (2001) Material supply to the abyssal seafloor in the Northeast Atlantic. Prog Oceanogr 50:27–63

Larkin K, Ruhl HA, Bagley P, Benn A and others (2010) Benthic biology time-series in the deep sea: indicators of change. Community white paper. In: Hall J, Harrison DE, Stammer D (eds) Proc OceanObs'09: Sustained ocean observations and information for society. European Space Agency, Noordwijk

Lecroart P, Maire O, Schmidt S, Grémare A, Anschutz P, Meysman FJR (2010) Bioturbation, short-lived radioisotopes, and the tracer-dependence of biodiffusion coefficients. Geochim Cosmochim Acta 74:6049–6063

Lohrer AM, Thrush SF, Hunt L, Hancock N, Lundquist C (2005) Rapid reworking of subtidal sediments by burrowing spatangoid urchins. J Exp Mar Biol Ecol 321:155–169

Maire O, Duchêne JC, Rosenberg R, Braga de Mendonça J Jr, Grémare A (2006) Effects of food availability on sediment reworking in *Abra ovata* and *A. nitida.* Mar Ecol Prog Ser 319:135–153

Maire O, Lecroart P, Meysman F, Rosenberg R, Duchêne JC, Grémare A (2008) Quantification of sediment reworking rates in bioturbation research: a review. Aquat Biol 2: 219–238

Martinell J, de Gibert JM, Domenech R, Ekdale AA, Steen PP (2001) Cretaceous ray traces? An alternative interpretation for the alleged dinosaur tracks of La Posa, Isona, NE Spain. Palaios 16:409–416

McCarthy MA (2007) Bayesian methods for ecology. Cambridge University Press, Cambridge

Meysman FJR, Middelburg JJ, Heip CHR (2006) Bioturbation: a fresh look at Darwin's last idea. Trends Ecol Evol 21:688–695

Meysman FJR, Malyuga VS, Boudreau BP, Middelburg JJ (2008a) A generalized stochastic approach to particle dispersal in soils and sediments. Geochim Cosmochim Acta 72:3460–3478

Meysman FJR, Malyuga VS, Boudreau BP, Middelburg JJ (2008b) Quantifying particle dispersal in aquatic sediments at short time scales: model selection. Aquat Biol 2: 239–254

Meysman FJR, Boudreau BP, Middelburg JJ (2010) When and why does bioturbation lead to diffusive mixing? J Mar Res 68:881–920

Norcross BL, Mueter FJ (1999) The use of an ROV in the study of juvenile flatfish. Fish Res 39:241–251

Purser A, Bergmann M, Lundalv T, Ontrup J, Nattkemper TW (2009) Use of machine-learning algorithms for the automated detection of cold-water coral habitats: a pilot study. Mar Ecol Prog Ser 397:241–251

Raymond EH, Widder EA (2007) Behavioral responses of two deep-sea fish species to red, far-red, and white light. Mar Ecol Prog Ser 350:291–298

Reed DC, Huang K, Boudreau BP, Meysman FJR (2006) Steady-state tracer dynamics in a lattice-automaton model of bioturbation. Geochim Cosmochim Acta 70: 5855–5867

Rhoads DC, Boyer LF (1982) The effect of marine benthos on physical properties of sediment: a successional perspective. In: McCall PL, Tevesz MJS (eds) Animal–sediment relations. Plenum Press, New York, NY, p 3–52

Robert K (2011) Methodological approaches to the optimization of observatory systems for the study of benthic ecological processes. MSc thesis, University of Victoria, Victoria, BC

Ruhl HA, Smith KL Jr (2004) Shifts in deep-sea community structure linked to climate and food supply. Science 305: 513–515

Salazar MH (1970) Phototaxis in the deep-sea urchin *Allocentrotus fragilis* (Jackson). J Exp Mar Biol Ecol 5: 254–264

Service RF (2007) Oceanography's third wave. Science 318: 1056–1058

Sherman AD, Smith KL (2009) Deep-sea benthic boundary layer communities and food supply: a long-term monitoring strategy. Deep-Sea Res II 56:1754–1762

Smith CR, Pope RH, DeMaster DJ, Magaard L (1993) Age-dependent mixing of deep-sea sediments. Geochim Cosmochim Acta 57:1473–1488

Smith KL Jr, Kaufmann RS (1999) Long-term discrepancy between food supply and demand in the deep eastern North Pacific. Science 284:1174–1177

Smith KL Jr, Kaufmann RS, Wakefield WW (1993) Mobile megafaunal activity monitored with a time-lapse camera in the abyssal North Pacific. Deep-Sea Res I 40: 2307–2324

Smith KL Jr, Ruhl HA, Kaufmann RS, Kahru M (2008) Tracing abyssal food supply back to upper-ocean processes over a 17-year time series in the northeast Pacific. Limnol Oceanogr 53:2655–2667

Smith KL Jr, Ruhl HA, Bett BJ, Billett DSM, Lampitt RS, Kaufmann RS (2009) Climate, carbon cycling, and deep-ocean ecosystems. Proc Natl Acad Sci USA 106: 19211–19218

Solan M, Germano JD, Rhoads DC, Smith C and others (2003) Towards a greater understanding of pattern, scale and process in marine benthic systems: a picture is worth a thousand worms. J Exp Mar Biol Ecol 285–286:313–338

Solan M, Wigham BD, Hudson IR, Kennedy R and others (2004) *In situ* quantification of bioturbation using time lapse fluorescent sediment profile imaging (f SPI), luminophore tracers and model simulation. Mar Ecol Prog Ser 271:1–12

Stephens PA, Buskirk SW, del Rio CM (2007) Inference in ecology and evolution. Trends Ecol Evol 22:192–197

Stoner AW, Spencer ML, Ryer CH (2007) Flatfish–habitat associations in Alaska nursery grounds: use of continuous video records for multi-scale spatial analysis. J Sea Res 57:137–150

Taylor R, Vine N, York A, Lerner S and others (2008) Evolution of a benthic imaging system from a towed camera to an automated habitat characterization system. In: Oceans '08 MTS/IEEE, 15–18 September 2008, Quebec City, QC, p 1–7

Teal LR, Bulling MT, Parker ER, Solan M (2008) Global patterns of bioturbation intensity and mixed depth of marine soft sediments. Aquat Biol 2:207–218

Thrush SF, Pridmore RD, Hewitt JE, Cummings VJ (1991) Impact of ray feeding disturbances on sandflat macrobenthos: Do communities dominated by polychaetes or shellfish respond differently? Mar Ecol Prog Ser 69:245–252

Vardaro MF, Ruhl HA, Smith KL Jr (2009) Climate variation, carbon flux, and bioturbation in the abyssal North Pacific. Limnol Oceanogr 54:2081–2088

Wakefield WW, Genin A (1987) The use of a Canadian (perspective) grid in deep-sea photography. Deep-Sea Res 34:469–478

Walther D, Edgington DR, Salamy KA, Risi M, Sherlock RE, Koch C (2003) Automated video analysis for oceanographic research. In: IEEE Computer Society Conference on Computer Vision and Pattern Recognition (CVPR), 16–22 June 2003, Madison, WI

Walther D, Edgington DR, Koch C (2004) Detection and tracking of objects in underwater video. In: IEEE Computer Society Conference on Computer Vision and Pattern Recognition (CVPR), 27 June–2 July 2004, Washington, DC, p I544–I549

Wheatcroft RA (1991) Conservative tracer study of horizontal sediment mixing rates in a bathyal basin, California borderland. J Mar Res 49:565–588

Wheatcroft RA, Jumars PA, Smith CR, Nowell ARM (1990) A mechanistic view of the particulate biodiffusion coefficient: step lengths, rest periods and transport directions. J Mar Res 48:177–207

Widder EA, Robison BH, Reisenbichler KR, Haddock SHD (2005) Using red light for *in situ* observations of deep-sea fishes. Deep-Sea Res I 52:2077–2085

Witte U (1999) Consumption of large carcasses by scavenger assemblages in the deep Arabian Sea: observations by baited camera. Mar Ecol Prog Ser 183:139–147

Yahel G, Yahel R, Katz T, Lazar B, Herut B, Tunnicliffe V (2008) Fish activity: a major mechanism for sediment resuspension and organic matter remineralization in coastal marine sediments. Mar Ecol Prog Ser 372:195–209

Editorial responsibility: Matthias Seaman, Oldendorf/Luhe, Germany

Submitted: April 15, 2011; Accepted: January 23, 2012
Proofs received from author(s): April 25, 2012